Measuring the Configurational Heat Capacity of Liquids

Li-Min Wang* and Ranko Richert

Department of Chemistry and Biochemistry, Arizona State University, Tempe, Arizona 85287-1604, USA

(Received 20 June 2007; published 31 October 2007)

A high electric field impedance experiment on supercooled molecular liquids is employed to transfer energy to the slow modes by absorption from the field and detect the increase of their ''configurational temperature'', T_{cfg}, via the change of the relaxation times. This allows us to determine the configurational heat capacity, which accounts for most of the excess heat capacity for stronger liquids, but for only half of the heat capacity step in the case of more fragile systems. It is also observed that T_{cfg} gradually approaches the phonon temperature on the structural relaxation time scale.

DOI: 10.1103/PhysRevLett.99.185701 PACS numbers: 64.70.Pf, 65.20.+w, 77.22.−d

Numerous materials of fundamental as well as technological interest are in their amorphous solid state of matter, and the glass transition is the most common route to achieving these glassy systems [1]. The glass transition is generally understood as being a purely kinetic effect, where at $T_{g,\mathrm{kin}}$ the relaxation time of the system matches the observation time window τ_g set by the experiment. A common approach to the value of T_g is by differential scanning calorimetry (DSC), where the onset of the heat capacity increase ΔC_p occurs at a temperature $T_{g,\mathrm{cal}}$ which is very close to the kinetic counterpart $T_{g,\mathrm{kin}}$. The rise of the liquid heat capacity (C_p^{liquid}) over the level of the crystal (C_p^{crystal}) or glass (C_p^{glass}) indicates the activity of slow configurational degrees of freedom which govern structural relaxations and viscous flow.

Above T_g the dynamics of glass-forming materials are characterized by nonexponential structural relaxations with a super-Arrhenius temperature dependence regarding their average relaxation time constant τ [2]. This temperature dependence is found to follow the Vogel-Fulcher-Tammann (VFT) law, $\log_{10}(\tau/s) = A + B/(T - T_0)$, but the origin of this behavior remains to be clarified. By extrapolation, the Vogel temperature T_0 coincides with the Kauzmann temperature T_K at which the excess entropy S_{exc} is zero, where $dS_{\mathrm{exc}} = \Delta C_p d\ln T$ with $\Delta C_p = C_p^{\mathrm{liquid}} - C_p^{\mathrm{crystal}}$ [3]. A more quantitative link between entropy and relaxation time has emerged from the picture of cooperatively rearranging regions (CRR's), and the relation reported by Adam and Gibbs (AG) reads

$$\log_{10}(\tau/s) = A + \frac{C}{TS_{\mathrm{cfg}}(T)}, \qquad (1)$$

where $S_{\mathrm{cfg}}(T)$ is the configurational entropy [4]. The commonly found temperature dependence for the excess entropy, $S_{\mathrm{exc}}(T) = S_\infty(1 - T_K/T)$ [5], results in VFT behavior if inserted into the AG relation as $S_{\mathrm{cfg}}(T) \approx S_{\mathrm{exc}}(T)$, demonstrating that the exhaustion of S_{cfg} explains the dramatically increasing relaxation times near T_g [6]. While the configurational contributions to C_p and S are essential quantities for rationalizing the glass transition of supercooled liquids, only the excess values can be measured directly, i.e., the values of the liquid over the crystal (or extrapolated glass) levels. It has been suggested already by Goldstein in 1976 that vibrational modes could be substantial contributions to the excess entropy and heat capacity [7]. Later, various approaches to this issue have suggested that only a fraction of the excess entropy is of configurational nature [8–11]. Possible pictures of the configurational contribution to entropy $S(T)$ and heat capacity $C_p(T)$ have been supplied earlier [8,12]. These studies state that the configurational contribution is not directly accessible by experiment, but provide estimates on the quantities involved, partly relying on particular models which have been criticized [13]. Also, no agreement is obtained on how the fraction of vibrational contributions might depend on fragility.

Temperature modulated DSC, dynamic heat capacity studies, and theoretical insight have shown that heat uptake occurs on a broad spectrum of time scales [14–16]. The relaxation time dispersion of $C_p(\omega)$ is often reminiscent of the distribution of structural relaxations observed by other techniques [17]. Common to these methods is that heat is initially provided to the phonon bath and subsequently transferred to the slower degrees of freedom [18]. Because possible vibrational contributions to the excess heat capacity are present only in the equilibrium state, these modes acquire heat from the phonon bath on the slow time scale of the structural relaxation and therefore will remain inseparable in these experiments. The aim of this Letter is to offer an experimental route to quantifying the configurational heat capacity of liquids rather directly. In these nonlinear dielectric experiments, the heat is absorbed directly by the slow modes from an external electric field and only the configurational heat capacity is relevant for the observed increase of the effective temperature [19–21]. Because vibrational and configurational modes remain decoupled on the time scale of this reversed calorimetric measurement, the concept of the present technique allows one to access the configurational heat capacity by experiment.

The liquids of this study, 1,2-pentanediol (12PD, 96%), 2,4-pentanediol (24PD, 98%), *N*-methylcaprolactam (NMEC, 99%), propylene carbonate (PC, 99.7% anhydrous), and D-sorbitol (SORB, 98%), are purchased from Aldrich and used as received. DSC traces are recorded with a Perkin-Elmer DSC-7 and a TA Intruments 2920, with typical errors below 5% regarding $C_p(T_g)$. Results for glycerol (GLY) [20] and propylene glycol (PG) [21] are from reanalyzing previous data. Samples are prepared between two brass electrodes (16 and 20 mm ∅), which are separated by a 10 μm thick Teflon ring and the cell is held at the desired temperature by a Novocontrol Quatro cryostat. The dielectric behavior, $\hat{\varepsilon}(\omega)$, is determined by a Solartron SI-1260 gain/phase analyzer as described previously [21], with the voltage amplified using a Trek PZD-700 to achieve fields E_0 ranging from 14 kV/cm to 283 kV/cm for frequencies ν between 0.5 Hz and 50 kHz. A field, $E(t) = E_0 \sin(\omega t)$, is applied for typically 10 cycles, followed by a long zero-field cooling period and by the lower voltage measurement using $E_0 = 14$ kV/cm. This protocol is designed to minimize transient effects while avoiding phonon bath heating, and all field induced changes are completely reversible. The results are shown as the change of the frequency resolved dielectric loss, $\Delta \ln\varepsilon'' = \Delta\varepsilon''/\varepsilon'' = [\varepsilon''(E \gg 0) - \varepsilon''(E \to 0)]/\varepsilon''$, relative to the low-field limit.

The field effects for a typical example, PC at $T = 166$ K, are provided as loss profiles in Fig. 1(a), which show a substantial increase at elevated frequencies by $\Delta \ln\varepsilon''$ reaching 20% at $E_0 = 177$ kV/cm, while the typical measurement error does not exceed 0.2%. The $E_0 = 14$ kV/cm case represents the low-field limit. The E^2 normalization of the spectra in Fig. 1(b) demonstrates that the magnitude of $\Delta \ln\varepsilon''$ scales with E^2, independent of frequency. The appearance of the $\Delta \ln\varepsilon''(\nu)$ curves is very similar for all materials of this study: there is practically no effect for frequencies below that of the loss peak, and an almost constant relative increase across the high frequency wing that scales with E^2. Furthermore, the $\Delta \ln\varepsilon''(\nu)$ curves shift with temperature as do the low-field loss curves $\varepsilon''(\nu)$. The main material specific aspect of the field effects are the overall magnitudes of $\Delta \ln\varepsilon''$, which are compiled as solid symbols in Fig. 2(a) in terms of the peak value of $\Delta \ln\varepsilon''(\nu)$ after quadratic field scaling to a common value of $E_0 = 100$ kV/cm. At this electric field, the peak relative increases in the dielectric loss assume values between 0.8% and 6.3%, the highest number corresponding to PC [see Fig. 1(b)].

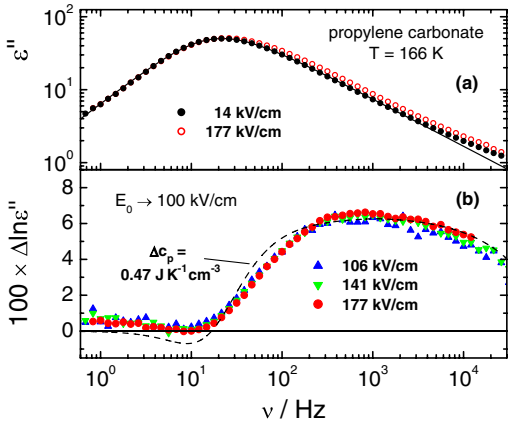

FIG. 1 (color online). Experimental results (symbols) for the frequency resolved dielectric loss, ε'', and its relative field induced change, $\Delta \ln\varepsilon''$, of propylene carbonate at $T = 166$ K. (a) The loss curves at high ($E_0 = 177$ kV/cm) and low ($E_0 = 14$ kV/cm) fields, together with an HN fit to the low-field data (line). (b) The relative changes, $\Delta \ln\varepsilon''$, for three different fields as indicated, but rescaled by E_0^2 towards a common field strength of $E_0^{\text{ref}} = 100$ kV/cm. The dashed lines reflect the calculation following Eq. (2), using $\Delta c_p = 0.47\ \text{J K}^{-1}\,\text{cm}^{-3}$. The relative signal increase reaches 20% at $E_0 = 177$ kV/cm.

In order to understand these field effects, we employ a model which originates from the rationale of dielectric hole-burning [22,23]. The approach rests on heterogeneous dynamics [24,25], i.e., dynamically distinct domains within which the dielectric, $\hat{\varepsilon}(\omega)$, and the thermal, $\hat{c}_p(\omega)$, relaxation proceeds exponentially with identical and locally correlated values for τ [19,20]. A sample of volume V will absorb the amount of $Q = \pi\varepsilon_0 E_0^2 \varepsilon''(\omega) V$ of energy from an external field, $E(t) = E_0 \sin(\omega t)$ [26]. For each domain, the energy gain term averaged over one period is given by the power $p = Q\omega/2\pi$, while the energy loss term is a matter of the thermal relaxation time with which the "configurational" temperature T_{cfg} approaches the phonon temperature T_{bath}. For steady state conditions, the time derivate of T_{cfg} is zero and the heat balance equation, $dT_{\text{cfg}}/dt = +p/c_p - T_{\text{cfg}}/\tau_T$, becomes $T_{\text{cfg}} = \tau_T p/c_p$ [20]. With the activation temperature T_A defined via $d\ln\tau/d(1/T) = T_A$, the net change of a local

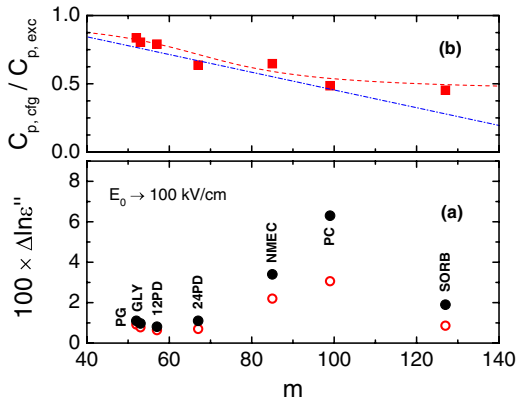

FIG. 2 (color online). Plateau values of the relative field induced change, $\Delta \ln\varepsilon''$, for different liquids sorted according to their fragility m: PG, GLY, 12PD, 24PD, NMEC, PC, and SORB. (a) Experimental results (solid symbols) and values calculated (open symbol) assuming $C_{p,\text{cfg}} = C_{p,\text{exc}}$. (b) Fraction of the configurational heat capacity, $C_{p,\text{cfg}}/C_{p,\text{exc}}$, as derived from the $\Delta \ln\varepsilon''$ results. The dashed line is a guide only, the dash-dotted line represents $(m - m_{\text{max}})/(m_{\text{min}} - m_{\text{max}})$.

time constant and the resulting susceptibility read

$$\ln\tau^* = \ln\tau - \frac{T_A}{T^2}\frac{\varepsilon_0 E_0^2 \Delta\varepsilon}{2\Delta c_p}\frac{\omega^2\tau^2}{1+\omega^2\tau^2}, \quad (2a)$$

$$\hat{\varepsilon}(\omega) = \varepsilon'(\omega) - i\varepsilon''(\omega) = \varepsilon_\infty + \Delta\varepsilon\int_0^\infty g(\tau)\frac{1}{1+i\omega\tau^*}d\tau, \quad (2b)$$

where ε_0 is the permittivity of vacuum and Δc_p is the configurational (volumetric) heat capacity. For a given frequency ω, the τ-dependent term in Eq. (2a) implies that domains associated with slower modes, $\tau \gg 1/\omega$, experience a significant increase of their T_{cfg}, while faster modes with $\tau \ll 1/\omega$ remain unchanged. The predicted plateau of $\Delta\ln\tau$ for $\tau \gg 1/\omega$ originates from the cancellation of two effects: domains with a more distant τ absorb less energy, but their rate of energy transfer to the bath is reduced accordingly. For frequencies ω below the loss peak of the sample, domains with $\tau > 1/\omega$ will not be found and the field effect thus disappears.

A quantitative application of Eq. (2) requires T_A, T, E_0, $\Delta\varepsilon$, Δc_p, and $g(\tau)$. Temperature T and field E_0 are given by the experimental conditions, the activation parameter T_A is determined from low-field data of the dielectric loss near T, $\Delta\varepsilon$, and $g(\tau)$ are derived from the low-field loss data using Havriliak-Negami fits, $\hat{\varepsilon}(\omega) = \varepsilon_\infty + \Delta\varepsilon[1 + (i\omega\tau)^\alpha]^{-\gamma}$. A representative example of how well the model captures the observed effects is included as the dashed line in Fig. 1(b), where a heat capacity value of $\Delta c_p = 0.47\ \mathrm{J\,K^{-1}\,cm^{-3}}$ was required in Eq. (2a) to account for the magnitude of the effect. An important observation is that this value of Δc_p represents only 49% of the measured heat capacity step at T_g [27]. It is gratifying to see that the reduction of $\Delta\ln\varepsilon''$ for higher frequencies is accounted for by the current model (see dashed line in Fig. 1(b) for $\nu > 1$ kHz), which is a direct consequence of the change in the slope $d\lg\varepsilon''/d\lg\nu$ (see data in Fig. 1(a) for $\nu > 1$ kHz).

The solid circles in Fig. 2(a) show the observed plateau values of $\Delta\ln\varepsilon''$ (normalized to a common field of $E_0 = 100$ kV/cm, but most data are taken between $E_0 = 70$ and 280 kV/cm where typical effects reached $\Delta\ln\varepsilon'' \approx 8\%$), while the open circles are the values predicted by Eq. (2) using the entire heat capacity step (glass-or-liquid step, as approximation to $c_{p,\mathrm{exc}}$) as seen in DSC experiments for Δc_p in Eq. (2a). The level for $\Delta\ln\varepsilon''$ predicted via $C_{p,\mathrm{cfg}}$ is always below the observed one, and the relative discrepancy increases with the fragility of the liquid, as has been anticipated [8]. Here, fragility is quantified by the steepness index m, defined as the slope in a fragility plot, $\log_{10}\langle\tau\rangle$ versus T_g/T, evaluated at $T = T_g$ [1,28]. The explanation for the above apparent discrepancy is straightforward: while DSC captures the total excess heat capacity, only its configurational contribution is relevant for the changes in the slow modes, for which we use the term configurational temperature T_{cfg}. Using $\Delta C_{p,\mathrm{cfg}}$ ($<\Delta C_{p,\mathrm{exc}}$) instead of $\Delta C_{p,\mathrm{exc}}$ will always lead to higher calculated values of the field effect. The square symbols in Fig. 2(b) compile the configurational fractions derived from this notion, $C_{p,\mathrm{cfg}}/C_{p,\mathrm{exc}}$, which range from 45% to 84%. Obviously, these fractions of $C_{p,\mathrm{cfg}}$ decrease systematically with fragility m, with both dashed lines being possible scenarios: saturation around 50% or linear disappearance between minimum ($m_{\mathrm{min}} = 16$) [28] and maximum ($m_{\mathrm{max}} = 170$) [27] values of fragility.

Consistent with Goldstein's assessment of the contributions to C_p above T_g [7], the configurational contribution $C_{p,\mathrm{cfg}}$ to the excess heat capacity is reduced to approximately 50% towards more fragile liquid, as shown in Fig. 2. Previous estimates on these quantities have provided fractions between 50% and 100%, without a consensus of how fragility affects these values. For selenium, $S_{\mathrm{cfg}}/S_{\mathrm{exc}} \approx 0.7$ has been derived from the density of states inferred from inelastic neutron scattering data [10]. Similar values for $S_{\mathrm{cfg}}/S_{\mathrm{exc}}$ are obtained for various liquids from comparing dynamic and thermodynamics data on the basis of the AG approach, Eq. (1), with pressure as an additional variable [9,11]. For *o*-terphenyl, it had been assumed that any excess vibrational heat capacity is absent in the liquid state and for the entropy this leads to estimating $S_{\mathrm{cfg}}/S_{\mathrm{exc}} = 0.81$ at T_g [29]. More recently, Johari attempted to identify the fraction of $C_{p,\mathrm{cfg}}/C_{p,\mathrm{exc}}$ by comparing DSC and dynamic heat capacity data under the premise that the two effects are separable on the time or frequency scale [30]. However, the excess vibrational modes of C_p contribute only in the equilibrium case;, i.e., they are associated with the slow time scales of the configurational modes, and thus will not display a plateau at frequencies in excess of the $C_p'(\omega)$ step. Generally, thermodynamic experiments that provide heat to the phonon bath, such as the dynamic C_p measurements, will observe that energy is lost to the slow degrees of freedom, but the nature of these slow modes will remain obscured. In the present experimental approach, however, energy is absorbed directly by the configurational degrees of freedom and remains decoupled from vibrational modes for the time scales of the structural (α-) relaxation process.

In the above analysis, it has been assumed that T_{cfg} of a particular domain relaxes to T_{bath} on the time scale of its structural relaxation. The implied persistence time of T_{cfg} and of the $\Delta\ln\varepsilon''$ effect is observed for PC at $T = 166$ K by recording the voltage, $V(t)$, and current, $I(t)$, signals during a high to low-field transition with a Nicolet Sigma 100 digital storage oscilloscope. At a frequency of $\nu = 1$ kHz, the signals are recorded every 2 μs with 14 bit resolution for a time period of 2 s. The inset of Fig. 3 depicts the raw current data for the ≈ 9 periods following the field change. The time resolved loss tangent is derived using $\tan(\delta) = \tan(\pi/2 - \Delta\varphi)$ from the phases φ of the $V(t)$ and $I(t)$ signals, evaluated by integration over individual periods preceding and following the transition from

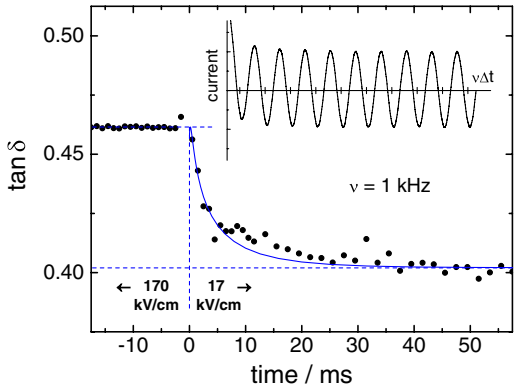

FIG. 3 (color online). Experimental results (symbols) for the loss tangent of propylene carbonate at $T = 166$ K. The value of $\tan\delta$ is evaluated for individual periods of a frequency of $\nu = 1$ kHz prior to and following a change in the electric field amplitude from $E_0 = 170$ kV/cm to $E_0 = 17$ kV/cm at $t = 0$. The solid curve is derived from the model as described in the text. The inset displays the ≈ 9 periods of current signal immediately following the decrease in field strength. For this inset, a sliding average over 70 μs has been applied to reduce noise.

$E_0 = 170$ kV/cm to $E_0 = 17$ kV/cm at $t = 0$ (equivalent to reducing Q by 100). The loss tangent, $\tan\delta$, at the higher field is 0.462, i.e., 14.8% above the value of 0.402 found at the low-field for long times, consistent with Eq. (2) predicting 14.7%. The interesting feature is that the response of $\tan\delta$ extends over 50 periods of the harmonic signals, as demonstrated in Fig. 3.

It remains to show that the nonexponential time evolution of $\tan\delta$ in Fig. 3 is consistent with the above model. In order to calculate the effect, it is assumed in Eq. (2a) and supported by hole-burning studies [19,23] that the net effect of $T_{\rm cfg} > T_{\rm bath}$, $\ln(\tau*/\tau)$, decays exponentially with a time constant of τ for each domain. The solid line in Fig. 3 reflects this calculation, lending strong support to the current model and leaving the relation between configurational and excess heat capacity the only uncertain quantity in Eq. (2).

In summary, large external time dependent fields are used to transfer energy to the configurational degrees of freedom and the change in configurational temperature, $T_{\rm cfg}$, is detected in terms of the dielectric susceptibility prior to its equilibration with vibrational modes. This allows a rather direct evaluation of the configurational contribution to excess heat capacities, $C_{p,\rm cfg}/C_{p,\rm exc}$, and entropies in supercooled liquids. For various molecular liquids it is found that $C_{p,\rm cfg}/C_{p,\rm exc}$ varies systematically from 84% to 45% with increasing fragility m. A time resolved measurement shows that $T_{\rm cfg}$ equilibrates on the time scale of the structural relaxation, independent of fragility.

The authors are grateful to C. A. Angell and D. V. Matyushov for valuable comments, and to J.-P. Belières for help with the DSC. Acknowledgment is made to the donors of the American Chemical Society Petroleum Research Fund (ACS-PRF) for support of this research under Grant No. 42364-AC7.

*Permanent address: State Key Lab of Metastable Materials Science and Technology, and College of Materials Science and Engineering, Yanshan University, Qinhuangdao, Hebei, 066004 China.

[1] C. A. Angell, K. L. Ngai, G. B. McKenna, P. F. McMillan, and S. W. Martin, J. Appl. Phys. **88**, 3113 (2000).
[2] J. C. Dyre, Rev. Mod. Phys. **78**, 953 (2006).
[3] C. A. Angell, J. Res. Natl. Inst. Stand. Technol. **102**, 171 (1997).
[4] G. Adam and J. H. Gibbs, J. Chem. Phys. **43**, 139 (1965).
[5] W. Kauzmann, Chem. Rev. **43**, 219 (1948).
[6] R. Richert and C. A. Angell, J. Chem. Phys. **108**, 9016 (1998).
[7] M. Goldstein, J. Chem. Phys. **64**, 4767 (1976).
[8] L.-M. Martinez and C. A. Angell, Nature (London) **410**, 663 (2001).
[9] D. Prevosto, M. Lucchesi, S. Capaccioli, R. Casalini, and P. A. Rolla, Phys. Rev. B **67**, 174202 (2003).
[10] W. A. Phillips, U. Buchenau, N. Nücker, A.-J. Dianoux, and W. Petry, Phys. Rev. Lett. **63**, 2381 (1989).
[11] S. Corezzi, L. Comez, and D. Fioretto, Eur. Phys. J. E **14**, 143 (2004).
[12] C. A. Angell, L.-M. Wang, S. Mossa, Y. Yue, and J. R. D. Copley, in *Slow Dynamics in Complex Systems, 3rd International Symposium*, edited by M. Tokuyama and I. Oppenheim, AIP Conf. Proc. No. 708 (AIP, New York, 2004), p. 473.
[13] M. Goldstein, Phys. Rev. B **71**, 136201 (2005).
[14] N. O. Birge and S. R. Nagel, Phys. Rev. Lett. **54**, 2674 (1985).
[15] A. A. Minakov, S. A. Adamovsky, and C. Schick, Thermochim. Acta **403**, 89 (2003).
[16] T. Christensen, N. B. Olsen, and J. C. Dyre, Phys. Rev. E **75**, 041502 (2007).
[17] K. Schröter and E. Donth, J. Chem. Phys. **113**, 9101 (2000).
[18] P. Strehlow and M. Meißner, Physica (Amsterdam) **263–264B**, 273 (1999).
[19] K. R. Jeffrey, R. Richert, and K. Duvvuri, J. Chem. Phys. **119**, 6150 (2003).
[20] R. Richert and S. Weinstein, Phys. Rev. Lett. **97**, 095703 (2006).
[21] S. Weinstein and R. Richert, Phys. Rev. B **75**, 064302 (2007).
[22] B. Schiener, R. Böhmer, A. Loidl, and R. V. Chamberlin, Science **274**, 752 (1996).
[23] B. Schiener, R. V. Chamberlin, G. Diezemann, and R. Böhmer, J. Chem. Phys. **107**, 7746 (1997).
[24] M. D. Ediger, Annu. Rev. Phys. Chem. **51**, 99 (2000).
[25] R. Richert, J. Phys. Condens. Matter **14**, R703 (2002).
[26] H. Fröhlich, *Theory of Dielectrics* (Clarendon, Oxford, 1958).
[27] L.-M. Wang, C. A. Angell, and R. Richert, J. Chem. Phys. **125**, 074505 (2006).
[28] R. Böhmer, K. L. Ngai, C. A. Angell, and D. J. Plazek, J. Chem. Phys. **99**, 4201 (1993).
[29] G. P. Johari, J. Chem. Phys. **112**, 8958 (2000).
[30] G. P. Johari, J. Chem. Phys. **126**, 114901 (2007).